

# Actively-targeted LTVSPWY peptide-modified magnetic nanoparticles for tumor imaging

Li-Yong Jie<sup>1</sup>  
Li-Li Cai<sup>2</sup>  
Le-Jian Wang<sup>2</sup>  
Xiao-Ying Ying<sup>2</sup>  
Ri-Sheng Yu<sup>1</sup>  
Min-Ming Zhang<sup>1</sup>  
Yong-Zhong Du<sup>2</sup>

<sup>1</sup>Department of Radiology, The Second Affiliated Hospital, Zhejiang University School of Medicine, <sup>2</sup>College of Pharmaceutical Sciences, Zhejiang University, Hangzhou, People's Republic of China

Correspondence: Yong-Zhong Du  
College of Pharmaceutical Sciences,  
Zhejiang University, 866 Yuhangtang  
Road, Hangzhou 310058,  
People's Republic of China  
Tel +86 571 8820 8439  
Fax +86 571 8820 8439  
Email duyongzhong@zju.edu.cn

Min-Ming Zhang  
Department of Radiology, The Second  
Affiliated Hospital, Zhejiang University  
School of Medicine, Hangzhou  
310009, China  
Tel/Fax +86 571 87315255  
Email cjr.zhangminming@vip.163.com

**Background:** Magnetic resonance imaging (MRI) is widely used in modern clinical medicine as a diagnostic tool, and provides noninvasive and three-dimensional visualization of biological phenomena in living organisms with high spatial and temporal resolution. Therefore, considerable attention has been paid to magnetic nanoparticles as MRI contrast agents with efficient targeting ability and cellular internalization ability, which make it possible to offer higher contrast and information-rich images for detection of disease.

**Methods:** LTVSPWY peptide-modified PEGylated chitosan (LTVSPWY-PEG-CS) was synthesized by chemical reaction, and the chemical structure was confirmed by <sup>1</sup>H-NMR. LTVSPWY-PEG-CS-modified magnetic nanoparticles were prepared successfully using the solvent diffusion method. Their particle size, size distribution, and zeta potential were measured by dynamic light scattering and electrophoretic mobility, and their surface morphology was investigated by transmission electron microscopy. To investigate their selective targeting ability, the cellular uptake of the LTVSPWY-PEG-CS-modified magnetic nanoparticles was observed in a cocultured system of SKOV-3 cells which overexpress HER2 and A549 cells which are HER2-negative. The in vitro cytotoxicity of these nanoparticles in SKOV-3 and A549 cells was measured using the MTT method. The SKOV-3-bearing nude mouse model was used to investigate the tumor targeting ability of the magnetic nanoparticles in vivo.

**Results:** The average diameter and zeta potential of the LTVSPWY-PEG-CS-modified magnetic nanoparticles was  $267.3 \pm 23.4$  nm and  $30.5 \pm 7.0$  mV, respectively, with a narrow size distribution and spherical morphology. In vitro cytotoxicity tests demonstrated that these magnetic nanoparticles were carriers suitable for use in cancer diagnostics with low toxicity. With modification of the LTVSPWY homing peptide, magnetic nanoparticles could be selectively taken up by SKOV-3 cells overexpressing HER2 when cocultured with HER2-negative A549 cells. In vivo biodistribution results suggest that treatment with LTVSPWY-PEG-CS-modified magnetic nanoparticles/DiR enabled tumors to be identified and diagnosed more rapidly and efficiently in vivo.

**Conclusion:** LTVSPWY-PEG-CS-modified magnetic nanoparticles are a promising contrast agent for early detection of tumors overexpressing HER2 and further diagnostic application.

**Keywords:** LTVSPWY peptide, HER2, poly(ethylene glycol), chitosan, magnetic nanoparticles, tumor targeting

## Introduction

During recent decades, use of magnetic nanoparticles in biomedical applications, such as magnetic drug delivery, magnetic resonance imaging (MRI), and cell and tissue targeting, has drawn considerable attention due to their unique magnetic properties and relatively small size as biological entities.<sup>1</sup> The responsiveness of magnetic

nanoparticles to external magnetic fields is fully exploited when they are used as drug delivery systems, whereby chemotherapeutic drugs can be delivered to specific locations in the body with the aid of external magnetic fields, whilst minimizing their side effects in healthy cells or tissues.<sup>2-5</sup>

MRI is widely used in modern clinical medicine as a diagnostic tool, and enables noninvasive and three-dimensional visualization of biological phenomena in living organisms with high spatial and temporal resolution.<sup>6,7</sup> As a consequence, considerable attention has been paid to multifunctional magnetic nanoparticles as potentially attractive stimuli-responsive MRI contrast agents,<sup>8,9</sup> because their magnetism can be modulated by their dispersion state.<sup>10</sup> However, sometimes the contrast difference between the biological tissues under investigation is trivial due to poor cellular uptake and failure to provide a high contrast signal.<sup>11</sup> Therefore, a contrast agent with efficient targeting ability and cellular internalization ability is needed to provide higher contrast and information-rich images for disease detection.

Solid lipid nanoparticles, developed in the early 1990s, are composed of physiologically compatible lipid components which decrease the risk of acute and chronic toxicity. Compared with traditional drug carriers, solid lipid nanoparticles combine the advantages of polymeric nanoparticles and emulsions for drug delivery, including having low toxicity, good biocompatibility, and tumor targeting ability.<sup>12</sup> Prolonged presence of the contrast agent at the target site is the primary requisite of any effective delivery system used for tumor imaging and diagnosis. In this regard, the effects of coating solid lipid nanoparticles with hydrophilic and flexible macromolecules such as poly(ethylene glycol) (PEG) to achieve a longer circulation time has been investigated.<sup>13-15</sup> Moreover, for enhancing solid lipid nanoparticles as an imaging probe, it has been necessary to modify the surfaces of solid lipid nanoparticles with a ligand to facilitate selective targeting of cancer cells more efficiently without loss of affinity and specificity. Human epidermal growth factor receptor 2 (HER2, also known as ErbB2, c-erbB2 or HER2/neu), plays an essential role in proliferation and antiapoptosis mechanisms in HER2-positive breast cancer.<sup>16</sup> LTVSPWY, a homing peptide which was identified using a biopanning procedure, has been reported to be able to deliver an antisense oligonucleotide selectively to HER2-positive tumor cells by conjugation with the oligonucleotide.<sup>17</sup>

Herein, we report the use of a lipid-modified magnetic nanoparticle as a model carrier to improve the sensitivity and selectivity of Fe<sub>3</sub>O<sub>4</sub>-based MRI contrast agents.

To achieve this, we synthesized LTVSPWY-modified PEGylated chitosan (LTVSPWY-PEG-CS), and then prepared and characterized LTVSPWY-PEG-CS-modified magnetic nanoparticles. Their average diameter, zeta potential, and surface morphology were investigated in detail. The tumor targeting ability of the modified magnetic nanoparticles when used as an MRI contrast agent was studied in vitro in a coculture system containing SKOV-3 cells which overexpress the cell surface marker HER-2 and A549 cells which are HER2-negative, and in vivo in an SKOV-3 tumor cell-bearing nude mouse model.

## Materials and methods

Chitosan with a molecular weight of 18.0 kDa was prepared by enzymatic degradation of chitosan (95% deacetylate, molecular weight 450 kDa) sourced from Yuhuan Marine Biochemistry Co, Ltd, Zhejiang, China, as in our previous work.<sup>18</sup> N,N'-disuccinimidyl carbonate (DSC) was purchased from Bio Basic Inc, Amherst NY. Di-tert-butyl dicarbonate [(Boc)<sub>2</sub>O], 1-ethyl-3-(3-dimethylaminopropyl) carbodiimide (EDC), and monostearin were purchased from Shanghai Medpep Co, Ltd, Shanghai, China. Oleic acid was purchased from Shuanglin Co, Ltd, Hangzhou, China. Trypsin and RPMI 1640 medium were purchased from Gibco BRL, Gaithersburg, MD. Fetal bovine serum was obtained from Hangzhou Sijiqing Biology Engineering Materials Co, Ltd, Hangzhou, China. Iron II, III oxide powder (Fe<sub>3</sub>O<sub>4</sub>, < 50 nm) and 3-(4,5-dimethylthiazol-2-yl)-2,5-diphenyltetrazolium bromide (MTT) were purchased from Sigma Chemical Co, St Louis, MO. Rhodamine B isothiocyanate (RITC) was also purchased from Sigma. Hoechst 33342 was obtained from Acros Organics, Fair Lawn, NJ. PKH67 fluorescent cell linker was sourced from Sigma. 1,1'-dioctadecyl-3,3',3'-tetramethyl indotricarbocyanine iodide (DiR) was purchased from Invitrogen, Grand Island, NY. All other reagents were analytical or chromatographic grade.

## Synthesis of LTVSPWY-PEG-CS copolymers

Briefly, 10 mg of LTVSPWY peptide was dissolved in dry dimethylformamide, and 3.1 μL (BOC)<sub>2</sub>O was added into the solution. The reaction was carried out for 24 hours at 40°C to protect the amine group in the LTVSPWY peptide. Next, 19.8 mg of EDC and 20.8 mg of NH<sub>2</sub>-PEG-NH<sub>2</sub> were added, followed by stirring at 40°C for 24 hours. After that, the reaction solution was reacted with N,N'-disuccinimidyl carbonate (NH<sub>2</sub>-PEG-NH<sub>2</sub>:DSC 1:1, mol/mol) for 12 hours at 40°C to obtain a succinimidyl t-Boc-LTVSPWY-PEG-NH<sub>2</sub> solution.

To obtain LTVSPWY-PEG-CS, chitosan was added into the reaction solution (chitosan:succinimidyl t-Boc-RGD-PEG-NH<sub>2</sub> 1:1, mol/mol) and the reaction was allowed to continue at 40°C for 24 hours. To stop protection of the LTVSPWY peptide by (BOC)<sub>2</sub>O, 3 M HCl was added and allowed to react for 2 hours. The pH of the reaction solution was then adjusted to 7.0 using 3 M NaOH. Finally, the reaction solution was dialyzed using a dialysis membrane (molecular weight cutoff 14 kDa; Spectrum Laboratories, Laguna Hills, CA) against distilled water for 24 hours, followed by lyophilization.

To obtain PEG-CS as a control, 200 mg of chitosan were dissolved in 30 mL of distilled water. Then, 55 mg of mPEG2000 with an aldehyde side group (PEG:chitosan 1:1, mol/mol) was added into the chitosan-SA solution. The solution was stirred overnight at room temperature and then dialyzed against distilled water using a dialysis membrane (molecular weight cutoff 7 kDa, Spectrum Laboratories) for 24 hours. The final product was lyophilized.

## Preparation of magnetic nanoparticles

Magnetic nanoparticles were prepared using the solvent diffusion method. Briefly, 5 mg of Fe<sub>3</sub>O<sub>4</sub> were added into 47 mL of 0.1% Poloxamer 188 in deionized water solution followed by sonication for 30 minutes using a probe sonicator (600 W, Sonicator JY92-II DN, Zhejiang, China) to form a dispersion of magnetic nanoparticles. To stabilize the nanoparticles, 1 mL of oleic acid in ethanol solution (5 mg/mL) was added and sonicated for 5 minutes. Next, 35 mg of monostearin was dissolved in 2 mL of dimethyl sulfoxide at 70°C and immediately injected into the aqueous dispersion of magnetic nanoparticles in an ultrasound waterbath at 70°C. The pre-emulsion was then cooled down to room temperature until magnetic nanoparticles were obtained.

To modify the magnetic nanoparticles further, an aqueous solution of LTVSPWY-PEG-CS (100 µg/mL) was added dropwise into the magnetic nanoparticle solution obtained under sonication using an ultrasound waterbath for 5 minutes to form LTVSPWY-PEG-CS-modified magnetic nanoparticles. As a control, PEG-CS or chitosan-modified magnetic nanoparticles were prepared as described above.

## Characteristics of magnetic nanoparticles

### <sup>1</sup>H NMR analysis of LTVSPWY-modified PEGylated chitosan

<sup>1</sup>H NMR spectra were used to analyze the synthesized LTVSPWY-PEG-CS. LTVSPWY, PEG2000, chitosan, PEG-CS, and LTVSPWY-PEG-CS were dissolved in D<sub>2</sub>O,

and measured using an NMR spectrometer (AC-80, Bruker Biospin, Germany).

### Determination of particle size, zeta potential, and TEM

The particle size and zeta potential of the magnetic nanoparticles were measured by dynamic light scattering using a Zetasizer (3000HS, Malvern Instruments Ltd, Worcestershire, UK). Morphological examination of the magnetic nanoparticles was performed using transmission electron microscopy (TEM, JEOL JEM-1230, Tokyo, Japan). The samples were stained with 2% (w/v) phosphotungstic acid and placed on copper grids with films for viewing.

## Cell culture

A SKOV-3 human ovarian carcinoma cell line and an A549 human lung carcinoma (alveolar type 2) cell line were obtained from the Cell Resource Center of the China Science Academy. The cells were cultured in RPMI 1640 medium at 37°C with 5% CO<sub>2</sub> under fully humidified conditions. All media were supplemented with 10% (v/v) fetal bovine serum, penicillin 100 U/mL, and streptomycin 100 U/mL. The cells were subcultured regularly using trypsin-ethylenediamine tetra-acetic acid.

## Cytotoxicity assay in vitro

A comparison of cytotoxicity was performed on the test cells with in vitro proliferation using the MTT method.<sup>19</sup> Briefly, SKOV-3 and A549 cells were plated in 96-well plates at a density of 1 × 10<sup>4</sup> cells/well in 200 µL of complete medium, and incubated for 24 hours to allow the cells to attach. The cells were then exposed to serial concentrations of magnetic nanoparticles at 37°C for 48 hours. At the end of incubation, 20 µL of the MTT solution was added, with incubation at 37°C for another 4 hours, and the medium was then replaced with 100 µL of dimethyl sulfoxide to dissolve the MTT formazan crystals. The plates were shaken for 10 minutes and absorbance was measured at 570 nm using a microplate reader (BioRad, Model 680, Hercules, CA).

## Competitive cellular uptake in vitro

Before incubation with the magnetic nanoparticles, the A549 cells were stained using a PKH67 fluorescent cell linker kit (Sigma), with the fluorescent cells becoming incorporated into the cell membrane with no modification of biological activity,<sup>20</sup> following the manufacturer's protocol with some modification. Briefly, the cells were resuspended

in 200  $\mu\text{L}$  diluent C, and then 200  $\mu\text{L}$  of PHK67 dye (4  $\mu\text{M}$ ) was added, followed by incubation for 10 minutes at room temperature. To stop the staining reaction, 1 mL of serum was added and incubated for 2 minutes, followed by centrifugation at  $400 \times g$  for 10 minutes. The cell pellet was washed twice more with 10 mL of complete medium to ensure removal of unbound dye and resuspended to the desired concentration.

The PKH67-labeled HER2-negative A549 cells were then cocultured with the HER2-overexpressing SKOV-3 cells<sup>21</sup> in the same well of a 24-well plate and incubated for 24 hours to allow attachment. The cells were then incubated with RITC-labeled magnetic nanoparticles (2:1, mol/mol) in growth medium for 12 hours. After washing the cells with phosphate-buffered solution three times, cellular uptake was observed using fluorescence microscopy (Olympus DP70, Melville, NY).

## Biodistribution of magnetic nanoparticles in vivo

Far-red or near-infrared light (spectral range 650–900 nm) provides a “clear” window for in vivo optical imaging because it is separated from the major absorption peaks of blood and water.<sup>22</sup> After optical calculations, we estimated that use of near-infrared-emitting DiR would improve tumor imaging sensitivity by at least ten-fold. DiR-loaded magnetic nanoparticles were prepared as described earlier, with some modifications. Briefly, a mixture of DiR and monostearin in dimethyl sulfoxide was injected into the aqueous dispersion of magnetic nanoparticles.

Tumor xenograft models were established by subcutaneous injection of approximately  $5 \times 10^6$  SKOV-3 cells in

100  $\mu\text{L}$  of serum-free RPMI 1640 medium into the flank of male BALB/C+nu/F1 nude mice. The mice were then subjected to imaging studies when their tumors had reached an acceptable size. After tail vein injection of DiR-loaded magnetic nanoparticles (with  $\text{Fe}_3\text{O}_4$ , oleic acid, monostearin, chitosan, and DiR concentrations of 50, 50, 350, 50, and 200  $\mu\text{g}/\text{mL}$ , respectively), the mice were anesthetized and imaged at multiple time points (1, 3, 6, 12, 24, 48, 72, and 96 hours) using Maestro in vivo imaging system (CRI Inc, Woburn, MA). The tunable filter was automatically stepped up in 10 nm increments from 580 nm to 700 nm while the camera captured images at each wavelength with constant exposure. Overall acquisition time was about 0.4 seconds. For ex vivo imaging, the tissues were subjected to fluorescence imaging using the Spectral system immediately after the tumors and organs were harvested.

## Statistical analysis

The data are expressed as the mean of three separate experiments. The statistical significance of the differences were determined using the Student's *t*-test for each paired experiment. A *P* value  $< 0.05$  was considered to be significant in all cases.

## Results and discussion

### Synthesis and characterization of LTVSPWY-PEG-CS

As shown in Figure 1, t-Boc-LTVSPWY-PEG-NH<sub>2</sub> was prepared by chemical reaction between the –COOH of LTVSPWY (its amino terminus preprotected by (Boc)<sub>2</sub>O) and the –NH<sub>2</sub> of NH<sub>2</sub>-PEG-NH<sub>2</sub> in the presence of EDC. t-Boc-LTVSPWY-PEG-CS was synthesized by conjugating the remaining amino

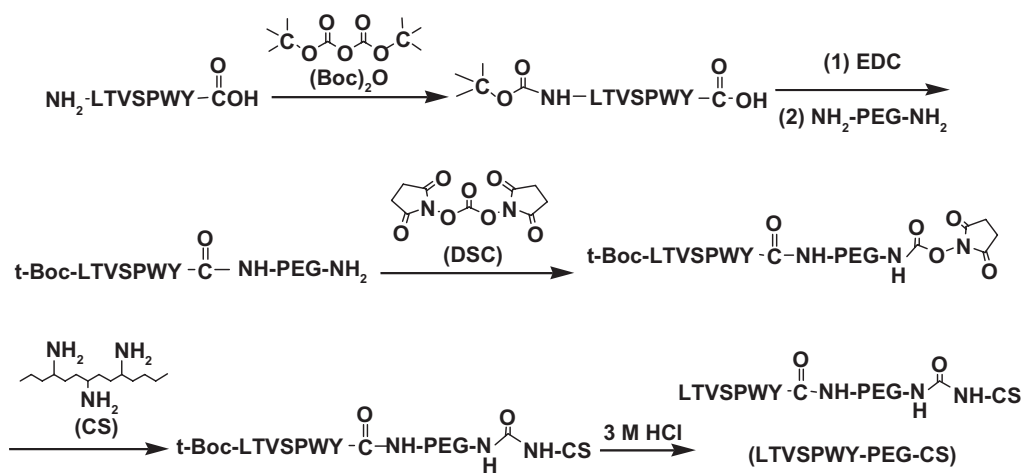


**Figure 1** Synthetic scheme of LTVSPWY-PEG-CS.

**Abbreviations:** PEG, poly(ethylene glycol); CS, chitosan.



**Table 1** Size and zeta potential of magnetic nanoparticles

Sample	Dn (nm)	PI (-)	Zeta potential (mV)
Non-modified MNPs	156.0 ± 11.5	0.19 ± 0.03	-10.4 ± 3.5
LTVSPWY-PEG-CS modified MNPs	267.3 ± 23.4	0.55 ± 0.14	30.5 ± 7.0
PEG-CS-modified MNPs	275.0 ± 59.4	0.48 ± 0.11	22.1 ± 0.8
CS-modified MNPs	278.3 ± 15.6	0.40 ± 0.09	23.1 ± 1.9

**Note:** Data represent the mean ± standard deviation (n = 3).

**Abbreviations:** MNPs, magnetic nanoparticles; PI, polydispersity index; dn, average diameter of magnetic nanoparticles; PEG, poly(ethylene glycol); CS, chitosan.

and chitosan-modified nanoparticles was reversed in the range of  $-10.4 \pm 3.7$  mV to  $30.5 \pm 7.0$  mV. This charge reversal indicates that the LTVSPWY-PEG-CS-modified magnetic nanoparticles had been prepared successfully. Figure 3 shows the size distribution and zeta potential of the LTVSPWY-PEG-CS-modified magnetic nanoparticles obtained by dynamic light scattering, suggesting that they had a narrow size distribution.

TEM is a powerful tool for detecting particle size and surface morphology in nanoparticles. The spherical morphology of our magnetic nanoparticles was confirmed by TEM (Figure 4). It was found that the particle size observed under TEM was smaller than that obtained by dynamic light scattering, which may be due to shrinkage of the inner core of the magnetic nanoparticles during the drying process needed when preparing samples for TEM.

### In vitro cytotoxicity assay

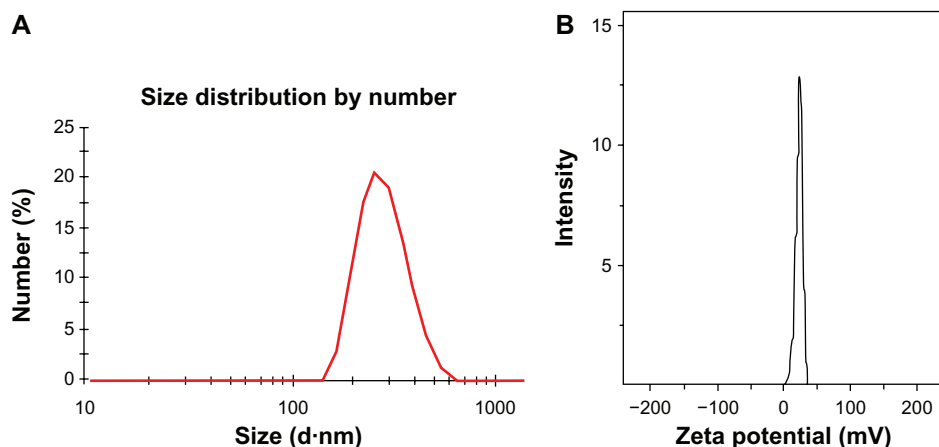
The cytotoxic effects of the magnetic nanoparticles against SKOV-3 and A549 cells was evaluated using the MTT test. Variations in cell viability according to nanoparticle

concentration are shown in Figure 5. Regardless of the increasing magnetic nanoparticle concentration, the viability of SKOV-3 and A549 cells remained above 80%, indicating that these nanoparticles would have low toxicity when used as carriers for cancer diagnostics.

### Competitive cellular uptake in vitro

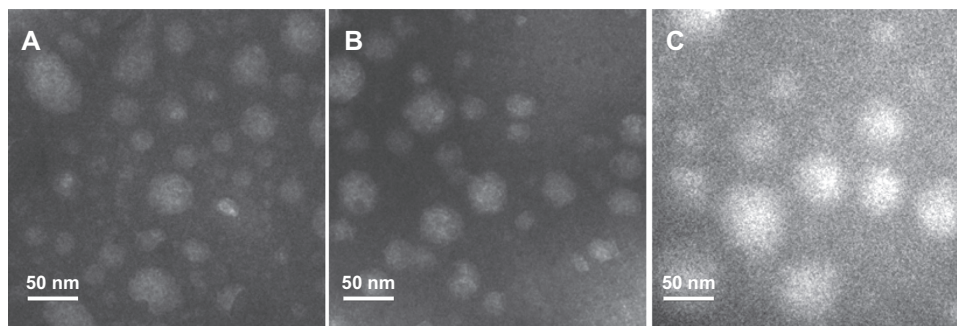
Using a coculture system containing SKOV-3 and A549 cells, the competitive cellular uptake of magnetic nanoparticles was investigated to determine the targeting ability of LTVSPWY-PEG-CS-modified magnetic nanoparticles toward SKOV-3 cells in vitro. The competitive cellular uptake was observed by fluorescence microscopy after the cells were incubated with LTVSPWY-PEG-CS-modified magnetic nanoparticles, PEG-CS-modified magnetic nanoparticles, or chitosan-modified magnetic nanoparticles for 12 hours. Figure 6 shows the fluorescence images of the effects of RITC-labeled magnetic nanoparticles in a cocultured system containing SKOV-3 and A549 cells.

Figure 6A shows clearly that there was a significant difference in uptake of LTVSPWY-PEG-CS-modified magnetic nanoparticles between SKOV-3 and A549 cells in the coculture system. Uptake of LTVSPWY-PEG-CS-modified magnetic nanoparticles by SKOV-3 cells was more efficient than by A549 cells, due to endocytosis mediated by the LTVSPWY homing peptide. However, the PEG-CS-modified magnetic nanoparticles showed similar uptake between SKOV-3 and A549 cells (Figure 6B), as did the chitosan-modified magnetic nanoparticles (Figure 6C). The competitive cellular uptake data confirm strong and specific binding of LTVSPWY-PEG-CS-modified magnetic nanoparticles with SKOV-3 cells, due to the abundant presence



**Figure 3** Characteristics of magnetic nanoparticles. Size distribution (A) and zeta potential (B) of LTVSPWY-PEG-CS-modified magnetic nanoparticles obtained by dynamic light scattering.

**Abbreviations:** PEG, poly(ethylene glycol); CS, chitosan.



**Figure 4** Transmission electron microscopic images of magnetic nanoparticles. **(A)** LTVSPWY-PEG-CS-modified magnetic nanoparticles, **(B)** PEG-CS-modified magnetic nanoparticles, and **(C)** CS-modified magnetic nanoparticles.

**Note:** The bar is 50 nm.

**Abbreviations:** PEG, poly(ethylene glycol); CS, chitosan.

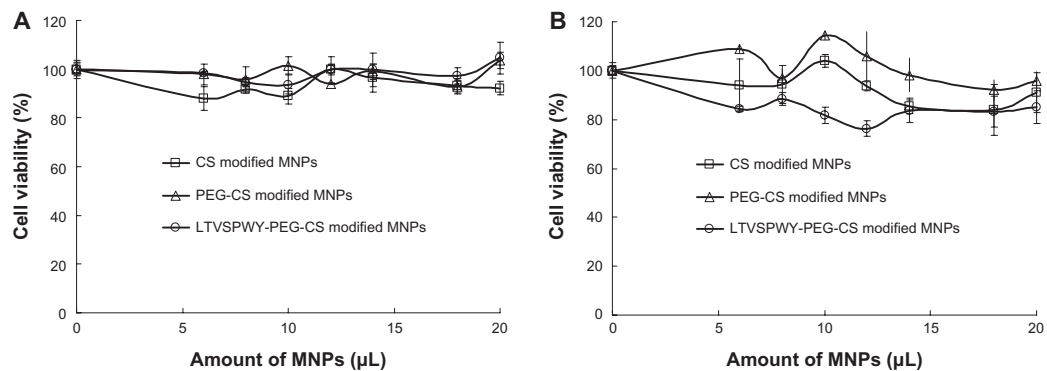


**Figure 5** Cytotoxicity of magnetic nanoparticles against A549 **(A)** and SKOV-3 **(B)** cells. The magnetic nanoparticles prepared consisted of 50 µg/mL  $Fe_3O_4$ , 50 µg/mL oleic acid, 350 µg/mL monostearin, and 50 µg/mL chitosan.

**Note:** Data represent the mean  $\pm$  standard deviation ( $n = 3$ ).

**Abbreviations:** PEG, poly(ethylene glycol); CS, chitosan.

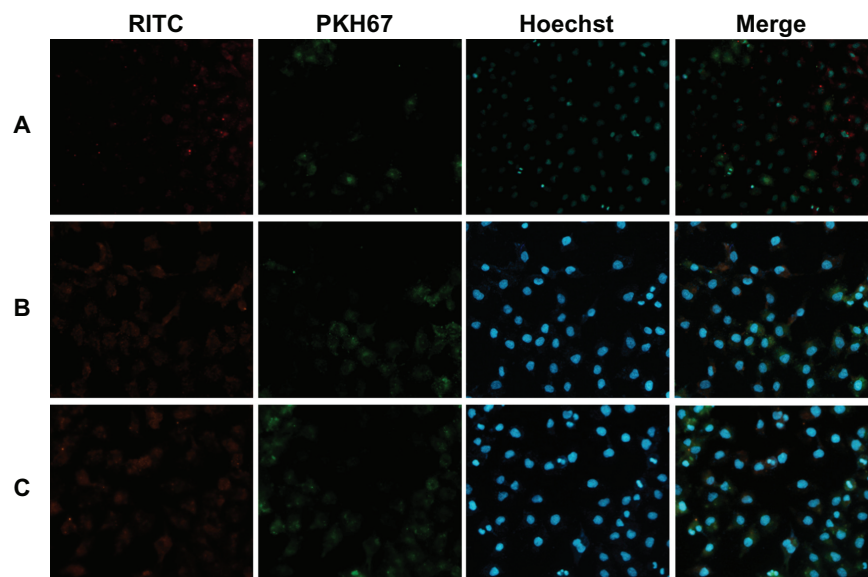


**Figure 6** Fluorescence images of competitive cellular uptake of RITC-labeled magnetic nanoparticles for 12 hours. A549 cells (HER2-negative, cytoplasmic membrane-labeled with PKH67 fluorescent linker, green) cocultured with HER2-overexpressing SKOV-3 cells were incubated with RITC-labeled magnetic nanoparticles (red). **(A)** LTVSPWY-PEG-CS-modified magnetic nanoparticles, **(B)** PEG-CS-modified magnetic nanoparticles, and **(C)** chitosan-modified magnetic nanoparticles.

**Note:** The cells were all stained with Hoechst 33342.

**Abbreviations:** RITC, rhodamine B isothiocyanate; PEG, poly(ethylene glycol); CS, chitosan.

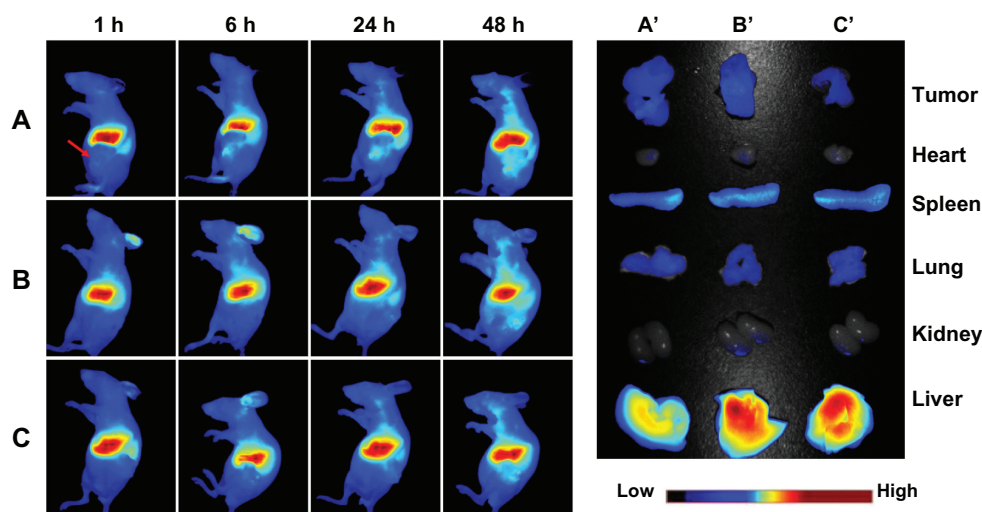


**Figure 7** In vivo and ex vivo biodistribution of DiR-loaded magnetic nanoparticles after intravenous tail injection in tumor-bearing nude mice. The fluorescent images of in vivo tumor-bearing nude mice (**A–B**) and ex vivo image of major organs (**A'–C'**) using DiR probes with three different magnetic nanoparticles, ie, (**A and A'**) LTVSPWY-PEG-CS-modified magnetic nanoparticles, (**B and B'**) PEG-CS-modified magnetic nanoparticles, and (**C and C'**) chitosan-modified magnetic nanoparticles.

**Notes:** The images were spectrally resolved. The tumor area is emphasized by a red arrow.

**Abbreviations:** PEG, poly(ethylene glycol); CS, chitosan.

of HER-2, a cell surface marker that is highly expressed by SKOV-3 cells.<sup>21</sup> These results confirm that LTVSPWY-PEG-CS-modified magnetic nanoparticles retain the binding activity and specificity of the LTVSPWY peptide, and may be used as an active targeting carrier via LTVSPWY peptide mediation.

### Biodistribution of magnetic nanoparticles in vivo

The in vivo behavior of the magnetic nanoparticles was then assessed following tail vein injection in a nude mouse model of a SKOV-3 xenograft in the left flank. The fluorescent images obtained at 1, 6, 24, and 48 hours after injection of DiR-loaded magnetic nanoparticles are shown in Figure 7. The uptake and retention of magnetic nanoparticles took place primarily in the liver, with little accumulation in tumor tissue. The maximum fluorescence signal is achieved at 48 hours after injection, and the tumor tissue is clearly delineated. Similar to the results obtained for cell uptake in vitro, more active accumulation of LTVSPWY-PEG-CS-modified magnetic nanoparticles was observed in a short time (one hour) within the area of the tumor (Figure 7A), in comparison with the PEG-CS-modified and chitosan-modified magnetic nanoparticles (Figure 7B and C). For PEG-CS-modified magnetic nanoparticles, the circulation time was increased, leading to slower accumulation of the magnetic nanoparticles in the tumors compared with the chitosan-modified magnetic nanoparticles.

Observation of the organs 96 hours after injection and dissection of the animals confirmed similar accumulation of LTVSPWY-PEG-CS-modified and PEG-CS-modified magnetic nanoparticles in the tumors. However, accumulation of LTVSPWY-PEG-CS-modified magnetic nanoparticles in the liver was reduced compared with that of the PEG-CS-modified and chitosan-modified ones. The biodistribution results obtained in this study indicate that modification by PEG, which prevents protein binding, can prolong the blood circulation time of the magnetic nanoparticles in vivo. More importantly, active tumor targeting using a tumor-specific ligand is much faster and more efficient than passive targeting based on tumor permeation, uptake, and retention.<sup>25</sup> Therefore, LTVSPWY-PEG-CS-modified magnetic nanoparticles can be delivered to tumors by both passive and active targeting mechanisms under in vivo conditions.

### Conclusion

In summary, LTVSPWY-PEG-CS-modified magnetic nanoparticles were successfully prepared using the solvent diffusion method. With modification by the LTVSPWY homing peptide, these magnetic nanoparticles could be taken up selectively by HER2-overexpressing SKOV-3 cells when cocultured with HER2-negative A549 cells, and with low toxicity. Treatment using LTVSPWY-PEG-CS-modified DiR-loaded magnetic nanoparticles enabled the tumors to be identified and diagnosed more rapidly and efficiently in vivo. Peptide-based nanoprobe may open up new opportunities



for the development of novel molecular imaging probes in the early detection and diagnosis of cancer.

## Acknowledgment

We are grateful for the financial support of the National Nature Science Foundation of China under contract 81171334 and Medical and health research funding schemes of Zhejiang Province under contract 2012KYB098.

## Disclosure

The authors report no conflicts of interest in this work.

## References

- Mahmoudi M, Simchi A, Imani M, et al. A new approach for the in vitro identification of the cytotoxicity of superparamagnetic iron oxide nanoparticles. *Colloids Surf B*. 2010;75(1):300–309.
- Polyak B, Friedman G. Magnetic targeting for site-specific drug delivery: applications and clinical potential. *Expert Opin Drug Deliv*. 2009;6(1):53–70.
- Lubbe AS, Alexiou C, Bergemann C. Clinical applications of magnetic drug targeting. *J Surg Res*. 2001;95(2):200–206.
- Gupta AK, Gupta M. Synthesis and surface engineering of iron oxide nanoparticles for biomedical applications. *Biomaterials*. 2005;26(18):3995–4021.
- Sunderland CJ, Steiert M, Talmadge JE, Derfus AM, Barry SE. Targeted nanoparticles for detecting and treating cancer. *Drug Dev Res*. 2006;67(1):70–93.
- Okada S, Mizukami S, Kikuchi K. Switchable MRI contrast agents based on morphological changes of pH-responsive polymers. *Bioorgan Med Chem*. 2012;20(2):769–774.
- Kaur S, Venkaraman G, Jain M, Senapati S, Garg PK, Batra SK. Recent trends in antibody-based oncologic imaging. *Cancer Lett*. 2012;315(2):97–111.
- Briley-Saebo K, Bjørnerud A, Grant D, Ahlstrom H, Berg T, Kindberg GM. Hepatic cellular distribution and degradation of iron oxide nanoparticles following single intravenous injection in rats: implications of magnetic resonance imaging. *Cell Tissue Res*. 2004;316(3):315–323.
- Singh A, Dilnawaz F, Mewar S, Sharma U, Jagannathan NR, Sahoo SK. Composite polymeric magnetic nanoparticles for co-delivery of hydrophobic and hydrophilic anticancer drugs and MRI imaging for cancer therapy. *ACS Appl Mater Interfaces*. 2011;3(3):842–856.
- Tanaka K, Kitamura N, Morita M, Inubushi T, Chujo Y. Assembly system of direct modified superparamagnetic iron oxide nanoparticles for target-specific MRI contrast agents. *Bioorg Med Chem Lett*. 2008;18(20):5463–5465.
- Corot C, Robert P, Idee JM, Port M. Recent advances in iron oxide nanocrystal technology for medical imaging. *Adv Drug Deliv Rev*. 2006;58(14):1471–1504.
- Sarmento B, Mazzaglia D, Bonferoni MC, Neto AP, Monteiro MC, Seabra V. Effect of chitosan coating in overcoming the phagocytosis of insulin loaded solid lipid nanoparticles by mononuclear phagocyte system. *Carbohydr Polym*. 2011;84(3):919–925.
- Gao JQ, Eto Y, Yoshioka Y, et al. Effective tumor targeted gene transfer using PEGylated adenovirus vector via systemic administration. *J Control Release*. 2007;122(1):102–110.
- Inada Y, Furukawa M, Sasaki H, et al. Biomedical and biotechnological applications of PEG- and PM-modified proteins. *Trends Biotechnol*. 1995;13(3):86–91.
- Hong JW, Park JH, Huh KM, Chung H, Kwon IC, Jeong SY. PEGylated polyethylenimine for in vivo local gene delivery based on lipiodolized emulsion system. *J Control Release*. 2004;99(1):167–176.
- Tai W, Mahato R, Cheng K. The role of HER2 in cancer therapy and targeted drug delivery. *J Control Release*. 2010;146(3):264–275.
- Shadidi M, Sioud M. Identification of novel carrier peptides for the specific delivery of therapeutics into cancer cells. *FASEB J*. 2003;17(2):256–258.
- Hu FQ, Ren GF, Yuan H, Du YZ, Zeng S. Shell cross-linked stearic acid grafted chitosan oligosaccharide self-aggregated micelles for controlled release of paclitaxel. *Colloids Surf B*. 2005;50(2):97–103.
- Mosmann T. Rapid colorimetric assay for cellular growth and survival: application to proliferation and cytotoxicity assays. *J Immunol Methods*. 1983;65(1–2):55–63.
- Martina MS, Wilhelm C, Lesieur S. The effect of magnetic targeting on the uptake of magnetic-fluid-loaded liposomes by human prostatic adenocarcinoma cells. *Biomaterials*. 2008;29(30):4137–4145.
- Lewis Phillips GD, Li G, Dugger DL, et al. Targeting HER2-positive breast cancer with trastuzumab-DM1, an antibody-cytotoxic drug conjugate. *Cancer Res*. 2008;68(22):9280–9290.
- Tziachristos V, Bremer C, Weissleder R. Fluorescence imaging with near-infrared light: new technological advances that enable in vivo molecular imaging. *Eur Radiol*. 2003;13(1):195–208.
- Boden N, Bushby RJ, Liu Q, et al. N'-Disuccinimidyl carbonate as a coupling agent in the synthesis of thiophospholipids used for anchoring biomembranes to gold surfaces. *Tetrahedron*. 1998;54(38):11537–11548.
- Ying XY, Du YZ, Hong LH, Yuan H, Hu FQ. Magnetic lipid nanoparticles loading doxorubicin for intracellular delivery: preparation and characteristics. *J Magn Magn Mater*. 2011;323(8):1088–1093.
- Gao X, Cui Y, Levenson RM, Chung LWK, Nie S. In vivo cancer targeting and imaging with semiconductor quantum dots. *Nat Biotechnol*. 2004;22(8):969–976.

International Journal of Nanomedicine

Publish your work in this journal

The International Journal of Nanomedicine is an international, peer-reviewed journal focusing on the application of nanotechnology in diagnostics, therapeutics, and drug delivery systems throughout the biomedical field. This journal is indexed on PubMed Central, MedLine, CAS, SciSearch®, Current Contents®/Clinical Medicine,

Submit your manuscript here: <http://www.dovepress.com/international-journal-of-nanomedicine-journal>

Dovepress

Journal Citation Reports/Science Edition, EMBase, Scopus and the Elsevier Bibliographic databases. The manuscript management system is completely online and includes a very quick and fair peer-review system, which is all easy to use. Visit <http://www.dovepress.com/testimonials.php> to read real quotes from published authors.